

Robust Control of Semi-passive Biped Dynamic Locomotion based on a Discrete Control Lyapunov Function

Chengju Liu[†], Jing Yang[†], Kang An^{‡*}, Ming Liu[¶]
and Qijun Chen[†]

[†] School of Electronics and Information Engineering, Tongji University, Shanghai, China.

E-mails: liuchengju@tongji.edu.cn, 1252583@tongji.edu.cn, qjchen@tongji.edu.cn

[‡] The College of Information, Mechanical and Electrical Engineering, Shanghai Normal University, Shanghai, China

[¶] Department of Computer Science & Engineering, the Hong Kong University of Science and Technology, Hong Kong, China. E-mail: eelium@ust.hk

(Accepted October 5, 2019)

SUMMARY

This paper focuses on robust control of a simplest passive model, which is established on a DCLF (discrete control Lyapunov function)-based control system, and presents gait transition method based on the study of purely passive walker. Firstly, the DCLF is introduced to stabilize walking process between steps exponentially by modulating the length of next step. Next, the swing leg trajectory from mid-stance position to foot-strike can be planned. Then the control law is calculated to resist external disturbance. Besides, an impulse is added just before foot-strike to realize a periodic walking pattern on flat or uphill ground. With walking terrain varying, the robot can transit to an adaptive walking gait in a few steps. With different push or pull disturbances acting on hip joint and the robot gait transiting on a continuously slope-changing downhill, the effectiveness of the presented DCLF-based method is verified using simulation experiments. The ability to walk on a changing environment is also presented by simulation results. The insights of this paper can help to develop a robust control method and adaptive walking of dynamic passive locomotion robots.

KEYWORDS: Biped robot; Semi-passive dynamic walking; Discrete control Lyapunov function (DCLF); Gait transition; Dynamic model.

1. Introduction

The biped robot has been brought into focus by its great terrain adaptability, obstacle avoiding ability and unlimited potential in the field of military, space and ocean exploration and emergency rescuing. Both the task-space and joint-space control methods have been studied.¹⁻⁵ The biped robot can realize the pre-defined walking pattern with active torque control methods,^{6,7} while the passive walker can present a human-like walking pattern on a declined slope depending only on its gravity changing and physical structure.^{8,9} To make best use of these two methods' advantages and bypass their disadvantages, the idea to combine the active control and passive walking is proposed, called passive-based control.¹⁰⁻¹²

Several researchers have proved the passive-based control can realize a more natural, robust and energy-saving walking pattern on different walking terrains with reasonable stability. H. Gritli et al. studied the semi-passive dynamic walking based on the OGY (OGY, Ott-Grebogi-Yorke) control approach. A torso-driven planar biped has been controlled to realize semi-passive gait and the bifurcations and chaos phenomenon has also been analyzed.^{12,14} Wang et al. introduced

* Corresponding author. E-mail: ankang526@foxmail.com

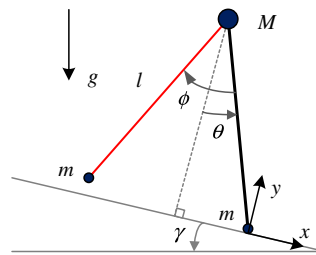


Fig. 1. Model of the biped simplest walker.

a torque-stiffness-controlled walking with an OGY-DFC control algorithm based on CPG.^{15,16} Large and small disturbance can be rejected by DFC and OGY method, respectively.^{17,18} The coordination among limb motions served as feedbacks to modulate the CPG model. The biped walker can realize stable and robust walking under different disturbances.^{19,20} Yildirim et al. analyzed and studied the characteristics of pure passive walking firstly.²¹ On this basis, the presented five-link robot can complete passive dynamic walking on level ground and inclined slope with a low energy-consumption.^{22,23} Fu et al. combined the CPG (central pattern generation) and passive walking to realize biped walking. Oscillators are directly utilized to control the hip and knee joints.^{24,25} During a walking cycle, the timing of the triggering and ceasing of oscillators were set by cognition of human practical walking.²⁶ Pranav et al. focused on the passive compass and the simplest walker and studied the features of passive walking gait. The gaits starting at timing of mid-stance and foot-striking were both studied.^{27,28} The dead-beat method and discrete control Lyapunov function were utilized to calculate the next step-length, which can be used to plan trajectory.^{28,29} Then the walking stability can be adapted exponentially within limited steps to realize robust walking patterns.^{30,31} In our previous work,^{32–34} some optimization methods have been used to generate a more energy-saving walking patterns on a downhill with the assumption that there is no external disturbance during the walking period. However, the external disturbance cannot be ignored in actual situation.

In this work, the DLCF-based control algorithm is presented to reject disturbance of the simplest walker. The passive-based gait transition method is proposed to generate more adaptive and energy-saving walking gaits. Comparing to the traditional robust controller, the presented controller is more energy-saving with the passive walking property. Besides, combined with the passive walking theory, the proposed gait-transition module can realize a more adaptive walking gait. Upon the theory analysis and simulation conducting, the algorithm presented here can obviate the push or pull disturbance acting on hip joint within a reasonable wide range and switch the simplest model to a more proper walking pattern. Then the robot can realize robust and adaptive walking gaits against external disturbances and changing of walking environment.

The remainder of the paper is organized as follows. Section 2 analyzes the biped model and walking gaits. Section 3 develops the control of biped robot based on DLCF. The approach is demonstrated to be validity in Section 4 with different simulations. The paper concludes in Section 5, including an outline of future work.

2. Biped Model

2.1. Model description

This paper deals with a planar walker model shown in Fig. 1, named simplest walker. The walker consists of two legs and three masses. The hip mass M is far greater than the mass m of foot, which means $m/M \rightarrow 0$. Besides, the length of leg is $l = 1$ and the initial downhill slope angle is $\gamma = 0.009$ rad. During the walking process, some assumptions are made as following. First, the friction between the robot and ground is sufficient so that there is neither rebounding nor sliding.^{33–35} Then, all the strikes are regarded as instantaneous and fully inelastic impacts. Last but not the least, there is no force between the ground and the stance leg which is about to leave the ground.

The simplest model was studied by Garcia *et al.*⁹ As Fig. 1 shows, the simplest model presents two sets of period-one walking solutions, a stable solution and an unstable solution respectively. With reasonable initial parameters, it can walk on inclined slopes without any external control torques. However, the application of passive walking is limited despite its sensitivity to parameters, which

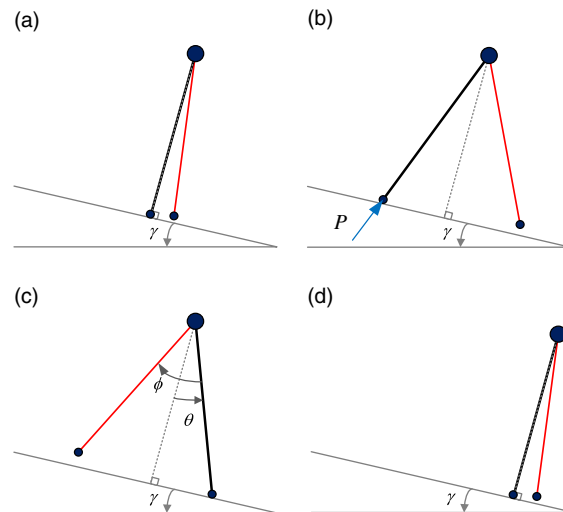


Fig. 2. Biped periodic gait starts at mid-stance.

leads to a poor adaptability for disturbances or environmental changing. The simplest walker is used to present a better insight to achieve a more clear and concise analysis of dynamic walking. Therefore, based on passive walking characteristics, the hip torque τ is added to overcome the deficit of sensitivity.

2.2. Gait analysis

An ideal walking pattern would be a gait that can converge to a stable mode by automotive perception and adaptive adjustment. Therefore, the analysis of biped walking gait is of great significance. The robot starts walking at the state $s_k(\theta, \phi)$, and then gets to the same state of next step $s_{k+1}(\theta, \phi)$. This period is called a walking cycle. Theoretically, the state $s_k(\theta, \phi)$ can be chosen as an arbitrary state during the walking.

The walking gait usually starts when the swing foot strikes the ground, namely the $s_k(\theta_{\text{init}}, \phi_{\text{init}})$ state and ends at the next foot-strike event. In this case, the walking process can be naturally divided into a continuous swing phase and a discrete foot-strike phase. Further, the Poincare return section is naturally chosen as the foot-strike event, and the Poincare return map serves as to search for the fixed point and the eigenvalues of the linearized return map which can explain the walking stability.

The mid-stance is the moment that the stance leg is vertical to the ground and it plays a critical role in robust walking and practical applications. The hip position reaches the highest position while angular velocity is the smallest and easy to measure at mid-stance. Besides, the hip angular velocity is critical for the analysis of robot falling events. If the hip velocity is much larger or smaller, the robot would easily fall forward or backward. In contrast, the walking gait starts at foot-strike events is not convenient for physical robot because it is hard to measure the impulse acting on the stance foot at this moment. Meanwhile, the gait starting at mid-stance contains the foot-strike as an independent phase and can be controlled by discrete control method.

The gait starting at mid-stance is shown as Fig. 2, in which the walking gait is divided into three phases. The first swing phase starts from a mid-stance and ends at the moment before foot-strike. The strike phase is the discrete foot-strike event. An impulse is added just before foot-strike to make it possible for the simplest robot to walk on a flat or even uphill slope, while there is no impulse added on a downhill. The second swing phase begins after foot-strike and ends at the next mid-stance moment. Therefore, a whole walking gait cycle consists of two swing phases divided by the mid-stance and a foot-strike phase.

2.3. Walking dynamics

In this section, the dynamic motion equations of the biped in sagittal plane model is derived. As Fig. 1 shown, the x -axis is supposed to be along the forward direction and the y -axis is vertical to the ground. The angle between two legs ϕ and the angle between stance leg and the norm of the slope θ

are introduced to describe the configuration of biped model in the coordinate space. Thus, the robot posture can be arranged in a generalized vector $q = [\theta; \phi]$. The dynamic equation in swing phase can be obtained through the Lagrange's equation

$$D(q)\ddot{q} + H(q, \dot{q}) + G(q, \gamma) = u \quad (1)$$

where the matrices $D(q)$ and $H(q, \dot{q})$ are related to inertia and coriolis with centrifugal force respectively. The $G(q, \gamma)$ is the gravity matrix depending on the slope angle γ . The joint torque vector is presented as $u = [\tau; 0]$, which means that only the hip joint is controlled.

By letting $x = [q; \dot{q}]$, the formula (1) can be converted as formula (2) in the state space.

$$\dot{x} = \frac{d}{dt} \begin{bmatrix} q \\ \dot{q} \end{bmatrix} = f(x) + g(x)u \quad (2)$$

where $f(x)$ and $g(x)$ can be described as below

$$f(x) = \begin{bmatrix} \dot{q} \\ -D^{-1}(q)(H(q, \dot{q}) + G(q, \gamma)) \end{bmatrix} \quad (3)$$

$$g(x) = \begin{bmatrix} 0 \\ D^{-1}(q) \end{bmatrix}$$

With the assumption $m/M \rightarrow 0$, the model described in formula (3) can be simplified by rescaling time with $\sqrt{l/g}$. The dynamic equation during swing phase can be derived

$$\begin{aligned} \ddot{\theta} &= \sin(\theta - \gamma) \\ \ddot{\phi} &= \sin(\phi) (\dot{\theta}^2 - \cos(\theta - \gamma)) + \sin(\theta - \gamma) - \tau \end{aligned} \quad (4)$$

The detection of foot-strike event comes at the first to derive dynamic model during the foot-strike phase. The foot-strike occurs when the state of robot in real-time meets the collision condition as formula (5). According to the position and posture before and after foot-strike, as Fig. 2(b) and (c) show, the angle switches as formula (6) described. Thus, the relation of angular velocity before and after foot-strike can be derived by the conservation of angular momentum with time rescaled by $\sqrt{l/g}$, as formula (7) shown.

$$c(q) = \phi^- - 2\theta^- = 0 \quad (5)$$

$$\begin{bmatrix} \theta^+ \\ \phi^+ \end{bmatrix} = \begin{bmatrix} 1 & -1 \\ 0 & -1 \end{bmatrix} \begin{bmatrix} \theta^- \\ \phi^- \end{bmatrix} \quad (6)$$

$$\begin{bmatrix} \dot{\theta}^+ \\ \dot{\phi}^+ \end{bmatrix} = \begin{bmatrix} \dot{\theta}^- \cos(\phi^-) + P \sin(\phi^-) \\ \dot{\theta}^- \cos(\phi^-) (1 - \cos(\phi^-)) + P \sin(\phi^-) (1 - \cos(\phi^-)) \end{bmatrix} \quad (7)$$

The foot-strike phase can be modeled as

$$x^+ = \Delta(x^-) \quad (8)$$

where $x^- = [q^-; \dot{q}^-]$ and $x^+ = [q^+; \dot{q}^+]$ are the state vectors before and after foot-strike. And $\Delta(x^-)$ can be expressed as below

$$\Delta(x^-) = \begin{bmatrix} \theta^- - \phi^- \\ -\phi^- \\ \dot{\theta}^- \cos(\phi^-) + P \sin(\phi^-) \\ \dot{\theta}^- \cos(\phi^-) (1 - \cos(\phi^-)) + P \sin(\phi^-) (1 - \cos(\phi^-)) \end{bmatrix}$$

Besides, some practical constraints should be added during the walking process to make it correct. First, the direction of hip angular velocity must be the same as the walking direction, otherwise the

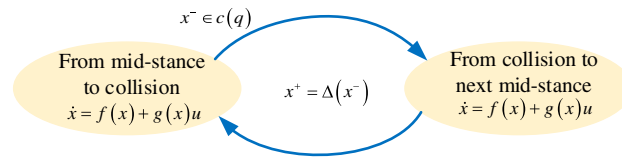


Fig. 3. Biped walking states switching diagram.

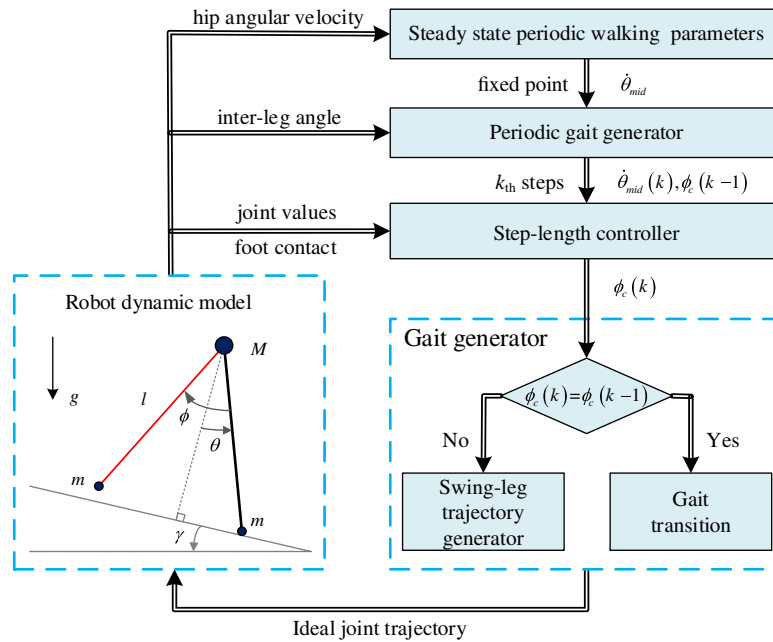


Fig. 4. Control diagram of the whole system.

robot will fall backward. Next, suppose that there is no flight phase which requires the direction of ground reaction force must be similar to the y direction. Combining with the configuration, the constraints can be described as follows

$$-\sqrt{\cos(\theta - \gamma)} < \dot{\theta} < 0 \tag{9}$$

With the dynamic model of swing phases, foot-strike phase and the physical constraints, the hybrid dynamic model of the simplest walker can be obtained.

$$\begin{aligned} \dot{x} &= f(x) + g(x)u, x^- \notin c \\ x^+ &= \Delta(x^-), x^- \in c \end{aligned} \tag{10}$$

where the state variable θ should meet the requirement expressed by formula (9). The symbol c represents the geometric constraints of foot-strike event. Figure 3 shows the walking gait is comprised of two swing phases and a foot-strike phase as formula (10) expressed.

3. Control Method

3.1. Outline of control system

This paper focuses on the simplest walking gait starting at mid-stance. During the period from mid-stance to foot-strike, a torque acting on hip joint is added to modulate the joint angle of swing leg. Therefore, the biped robot can resist push or pull disturbances. According to the analysis of purely passive walking and the solution of Poincare mapping, the biped walking on a changing slope can be realized by gait transition.

The architecture of control system is demonstrated as Fig. 4. The system consists of a parameter-input model, a periodic gait generator, a step-length controller and a gait generator.

The parameter-input model generates appropriate initial states and given parameters by solving Poincare mapping based on dynamics. The periodic gait generator is responsible for stable walking pattern generating. The step-length controller is based on Lyapunov stability theory. The controller is used to reject external disturbance and then improve the robustness of system. The gait generator begins with a judgement that determines whether there is external disturbance or not. If a disturbance is added, the step-controller can reject it and there is no need to transit gait. Otherwise, a new gait is generated. The step-length controller and gait generator are described in detail in the following subsections.

3.2. Step-length controller based on Lyapunov stability analysis

According to formula (4), the angle $\phi(t)$ between stance and swing leg can be completely controlled by hip torque τ while the angle $\theta(t)$ cannot be controlled during a walking period. However, based on the assumption $m \ll M$ and the dynamic model in formula (10), the state $\dot{\theta}_{\text{mid}}$ at mid-stance of every period is of great significance for the following walking process.

At the timing of mid-stance, a Lyapunov function is defined as formula (11) shown. Then the formula (12) can be derived to ensure the asymptotical stability of biped walking according to Lyapunov direct method. Furthermore, the Lyapunov exponent stability can be ensured by setting the exponent stability condition as formula (13) shown. Therefore, the angular velocity of stance can be controlled discretely to reach asymptotically stable.

$$V(\Delta\dot{\theta}_k) = \Delta\dot{\theta}_k^2 = (\dot{\theta}_k - \dot{\theta}_{\text{ideal}})^2 \quad (11)$$

$$V(\Delta\dot{\theta}_{k+1}) - V(\Delta\dot{\theta}_k) < 0 \quad (12)$$

$$V(\Delta\dot{\theta}_{k+1}) - V(\Delta\dot{\theta}_k) = -\lambda V(\Delta\dot{\theta}_k), 0 < \lambda < 1 \quad (13)$$

where λ is the exponent convergence rate. $\dot{\theta}_k$ and $\dot{\theta}_{\text{ideal}}$ denote the stance velocity and the ideal stance velocity at mid-stance in k -th step, respectively. $\dot{\theta}_0$ represents the given initial stance velocity. The formula (14) is the solution of the discrete equation (13). Then the relationship among the number of steps k , convergence rate λ , the size of external disturbance $|\dot{\theta}_0 - \dot{\theta}_{\text{ideal}}|$ and the convergence precision $|\dot{\theta}_k - \dot{\theta}_{\text{ideal}}|$ can be derived as formula (15).

$$V(\Delta\dot{\theta}_k) = V(\Delta\dot{\theta}_0) e^{-\lambda k}, 0 < \lambda < 1 \quad (14)$$

$$k = \frac{1}{\lambda} \ln \left(\frac{V(\Delta\dot{\theta}_0)}{V(\Delta\dot{\theta}_k)} \right) = \frac{2}{\lambda} \ln \left(\frac{|\dot{\theta}_0 - \dot{\theta}_{\text{ideal}}|}{|\dot{\theta}_k - \dot{\theta}_{\text{ideal}}|} \right) \quad (15)$$

According to formula (15), some analyses are conducted to demonstrate the interactions among parameters. As Fig. 5 shows, when $|\dot{\theta}_k - \dot{\theta}_{\text{ideal}}| = 0.005$ and $\dot{\theta}_{\text{ideal}} = -0.05923$, the interactions among k , λ and $\dot{\theta}_0$ can be analyzed. If $\dot{\theta}_0$ is determined, k is inversely proportional to the convergence rate λ . If the λ is chosen as a constant, k is proportional to the external disturbance acting on the robot $|\dot{\theta}_0 - \dot{\theta}_{\text{ideal}}|$. If k is set as a constant, the smaller the external disturbance, the wider the range of convergence rate λ is. When $\lambda < 0.2$, the low convergence rate leads to a large number of walking steps to reject disturbance. This situation cannot be applied in practice to make walking process stable rapidly. At the same time, when $\lambda > 0.7$, the number of walking steps is almost unaffected by λ if the external disturbance is small. If the λ is too large, the step-length controller can be seen as a dead-beat controller, which is sensitive to the model parameters. Therefore, the range of λ is chosen within $[0.2, 0.7]$ in the following simulations.

Then the local stability of robot walking can be studied by choosing the mid-stance state as Poincare section. Combining the conservation of energy with the switch of states before and after foot-strike, the analytic form of Poincare's mapping function can be expressed as follows

$$\dot{\theta}_{k+1} = F_1(\dot{\theta}_k, \phi_k^-, P_k, \gamma) \quad (16)$$

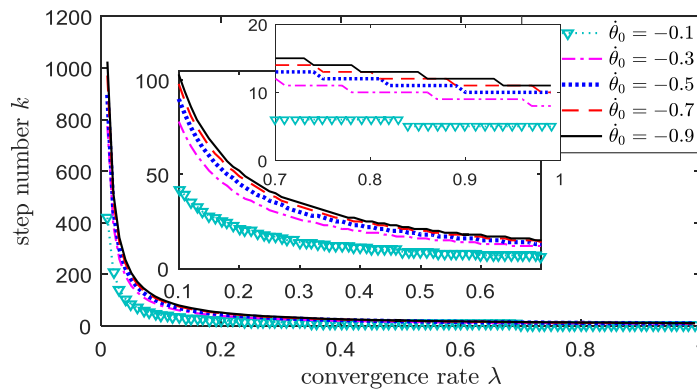


Fig. 5. The relationship between convergence rate and walking steps.

where ϕ_k^- is the ideal angle between swing and stance leg during the current gait, which is related to step length and therefore can be modulated to improve walking stability.

By solving the nonlinear equations (13) and (16), the step length related parameter ϕ_k^- can be calculated to make $\dot{\theta}_k$ converge to the given reference $\dot{\theta}_{\text{ideal}}$ at an exponent rate. From the practical point of view, by modulating the step length or the position of stance foot, the external disturbance can be rejected.

3.3. Swing leg trajectory planning

The value of ϕ_k^- that can keep the walking process stable exponentially is derived in above section. The stability between two successive steps can be guaranteed by modulating ϕ_k^- .

With the given initial states ϕ_0^m , $\dot{\phi}_0^m$ at initial given time $t = t_{\text{start}}$, and the definite value of and $\dot{\phi}_k^- = 0$ as end states at time $t = t_{\text{mid2strike}} + t_{\text{start}}$, the cubic interpolation method is applied to plan the trajectory of swing leg from mid-stance to foot-strike, where the walking time during this period $t_{\text{mid2strike}}$ can be predicted by formula (17).³¹ Then the swing leg trajectory can be planned by using a simple cubic interpolation. With the planned swing leg trajectory, the control torque used to realized robust walking can be derived according to the dynamic model in formula (4).

$$t_{\text{mid2strike}} = \int_{\theta=0}^{\theta=\frac{-\phi_k^-}{2}} \frac{d\theta}{\sqrt{(\dot{\theta}_k)^2 + 2(\cos \gamma - \cos(\theta - \gamma))}} \quad (17)$$

Therefore, the swing trajectory can guarantee that the stance angular velocity is anti-disturbance and exponentially stable during the following walking process.

3.4. Discrete control just before foot-strike for periodic walking

As Fig. 2 shows, a discrete impulse, named push-off, is added just before foot-strike to realize flat or uphill walking patterns based on the passive simplest model. As formula (16) presents the theory the conservation of energy with the switch of states before and after foot-strike. Combining the conservation of energy and the formula (8), the push-off at step k can be expressed as formula (18). By setting $\dot{\theta}_k = \dot{\theta}_{k+1} = \dot{\theta}_{\text{ideal}}$ and $\phi_k^- = \phi_{\text{ideal}}^-$, the push-off P_{ideal} can be obtained for a periodic walking pattern.

$$P_k = \frac{\cos(\phi_k^-) \sqrt{\dot{\theta}_k^2 + 2(\cos(\gamma) - \cos(\phi_k^-/2 - \gamma))} - \sqrt{\dot{\theta}_{k+1}^2 + 2(\cos(\gamma) - \cos(\phi_k^-/2 + \gamma))}}{\sin(\phi_k^-)} \quad (18)$$

By referring a typical human walking pattern, the nominal walking velocity $v_{\text{ideal}} = 1.30$ m/s is used to realize periodic walking on flat or uphill.^{27,36} With $v_{\text{ideal}} = 1.30$ m/s, the non-dimensional velocity can be calculated as $V_{\text{ideal}} = v_{\text{ideal}}/\sqrt{gl} = 1.30/\sqrt{10 \times 1} = 0.411$. Then the empirical fit³⁷ is utilized to get the step length, $SL_{\text{ideal}} = 1.25 \times V_{\text{ideal}}^{0.6} = 0.733$. The walking period time can be obtained by $T_{\text{ideal}} = SL_{\text{ideal}}/V_{\text{ideal}} = 1.783$. Combing the step-length with the physical robot model,

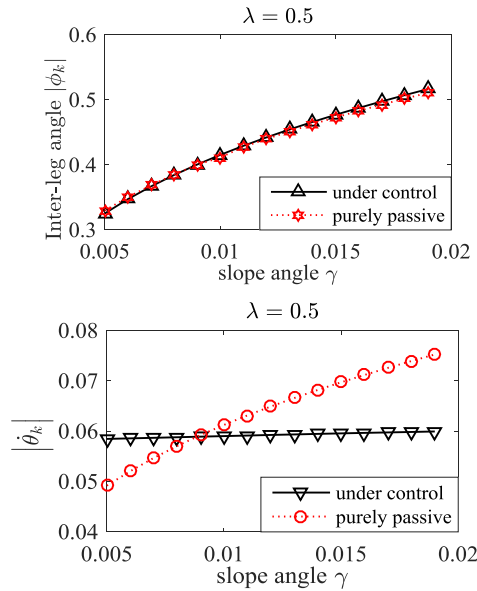


Fig. 6. The variation of step-length on different slopes.

the inter-leg angle ϕ_{ideal}^- can be calculated as -0.751 . Then the process to obtain $\dot{\theta}_{\text{ideal}}$ is described as following. Considering formula (17), which is the time period from mid-stance to foot-strike, the time period from foot-strike to the next mid-stance can be expressed as formula (19).

$$t_{\text{strike2mid}} = \int_{\theta = \frac{\phi_k^-}{2}}^{\theta = 0} \frac{d\theta}{\sqrt{(\dot{\theta}^+)^2 + 2(\cos(\phi^-/2 - \gamma) - \cos(\theta - \gamma))}} \quad (19)$$

According to $T_{\text{ideal}} = t_{\text{mid2strike}} + t_{\text{strike2mid}} = 1.783$ with energy conservation law, $\dot{\theta}_{\text{ideal}}$ (related with slope angle γ) can be calculated by a numerical method. Then the pushoff for changing slopes can be obtained online to realize a human-like walking pattern.

3.5. Gait transition

With the Lyapunov-based step-length controller, when $\dot{\theta}_0 = \dot{\theta}_{\text{ideal}}$ and $\lambda = 0.5$, the slope angle is assumed as a variable. Under the proposed control system, when the slope angle changes, the relationship between angle ϕ_k and swing angular velocity $\dot{\theta}_k$ can be presented in Fig. 6 as the black solid lines shown. Inspired by this phenomenon, the purely passive walking on the Poincaré Section of the simplest walker on different slopes are studied. Similarly, the relationship between ϕ_k and fixed point $\dot{\theta}_k$ is demonstrated in Fig. 6 as the red dotted lines shown. As Fig. 6 shows, the curves of inter-leg angle in these two situations are almost overlapped. However, the variations of $\dot{\theta}_k$ are not identical. Under the proposed control method, the value of $\dot{\theta}_k$ is almost a constant while $\dot{\theta}_k$ changes with slope angle in the purely passive walking. The reason why $\dot{\theta}_k$ is almost unchanged is that the Lyapunov-based step-length controller modulates $\dot{\theta}_k$ converge to a given ideal value exponentially. In this case, the tracking at exponent rate results in an unnatural walking gait and the unnecessary energy-consuming. Therefore, the gait transition on different walking slope is essential.

For the purely passive walking, combing the conservation of energy with the mapping expressed as formula (16), the relationships among ϕ_k , $\dot{\theta}_k$ and γ can be expressed theoretically as formula (20). The analytic solution of this mapping cannot be solved.

$$\phi_k = F_2(\dot{\theta}_k, \gamma) \quad (20)$$

The numerical simulations are conducted to present how the initial value $\dot{\theta}_k$ and slope angle γ effect the ϕ_k related to step length, as Fig. 7 shows.

In Fig. 7, when $\dot{\theta}_k$ is fixed as 0.05923, the variation of ϕ_k with γ is denoted as the blue triangle line. When γ is set as 0.009, the curve of ϕ_k with $\dot{\theta}_k$ is shown as the red circle line. As the Fig. 7 shows, in a reasonable range, the variation of $\dot{\theta}_k$ has few effects on ϕ_k while the variation of γ has

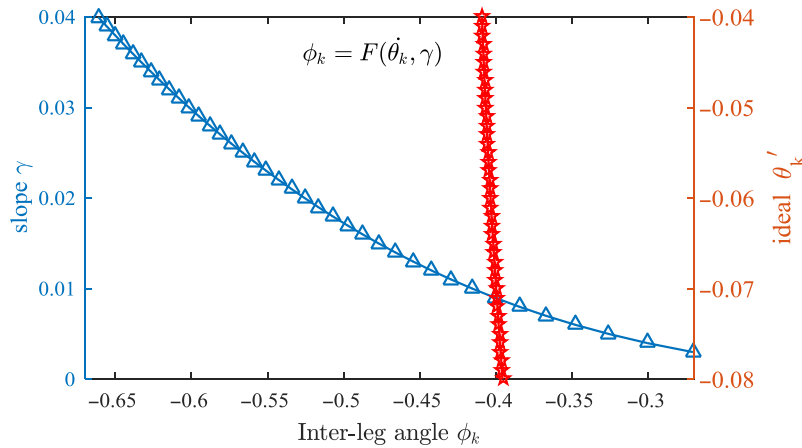


Fig. 7. The impacts of $\dot{\theta}_k$ and γ on the inter-leg angle in a reasonable range (purely passive).

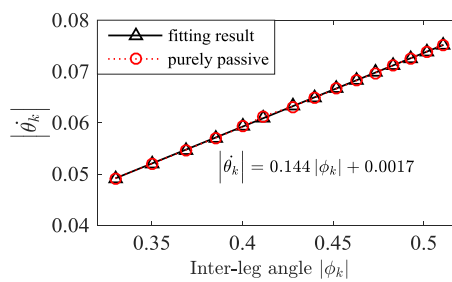


Fig. 8. The fitting result of purely passive walking.

great impact on ϕ_k . Therefore, the main factor affecting ϕ_k is the slope angle γ . This conclusion can better explain the result of Fig. 6 and ensure that the control method based on the above analysis is correct.

A gait transition process is added to the control system based on these theoretical analyses. The external disturbance must be rejected by using step-length controller firstly. Next, a fitting curve, as formula (21) expressed, is used to update the reference θ_{ideal} according to the real-time slope angle. Then the walking gait will transit to a more passive-like and energy-saving mode. The fitting curve is presented in Fig. 8, the primary polynomial fitting is good enough both in the simplicity and high-precision.

$$\dot{\theta}_{ideal} = - (0.144 |\phi_k^-| + 0.0017) \tag{21}$$

4. Simulation Results

4.1. Simulation 1- the exponential stability on the downhill

In this simulation, the validity of the presented control method is verified. The comparison between purely passive walking and the walking controlled by presented method with small disturbance is shown in Fig. 9. The black solid line represents purely passive walking, which is fluctuated greatly and easy to cause unstable walking.

Under the proposed control method, the disturbance can be rejected at an exponent rate and a much larger disturbance can be resisted, as Fig. 10 shown, where the horizontal cyan dotted line is the fixed point of purely passive walking. Therefore, the presented control method applied to the simplest walking can improve stability and enhance the capacity of resisting disturbance.

The size of disturbance that the control method can resist is analyzed as Fig. 10 shown. Both the above and below figures show, with the proposed control method, the robot can resist the push and pull disturbance, respectively. At different convergent rates, the number of steps needed to converge to the ideal value varies. This result is consistent with the previous theoretical analysis in Section 3.2.

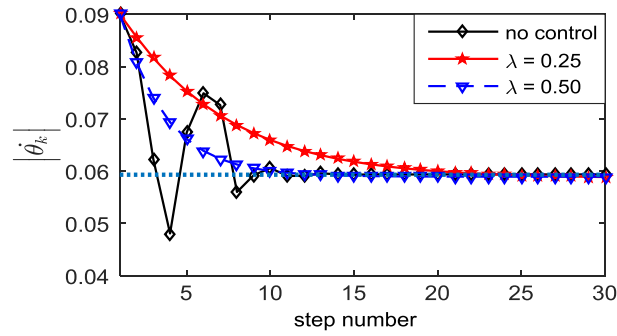


Fig. 9. Disturbance rejection with control V.S. without control.

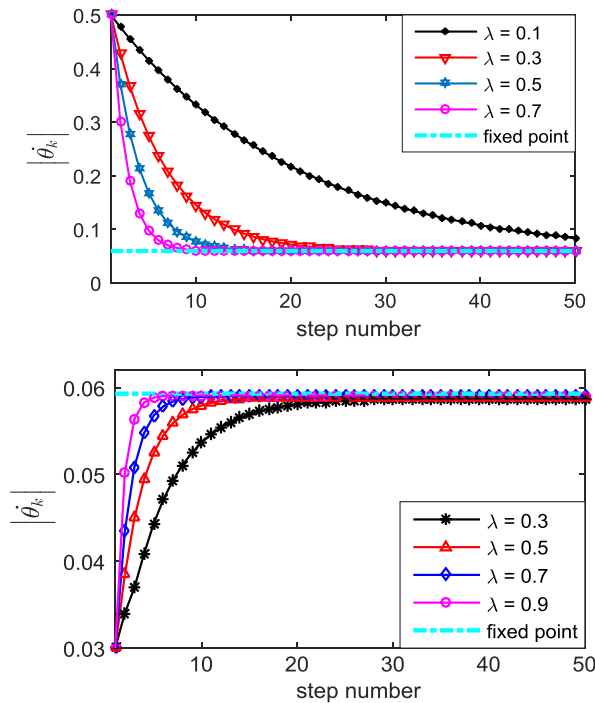


Fig. 10. Push and pull disturbance can be resisted.

The figures in Fig. 11 vary from the convergent rates and each figure shows the exponent convergence under different external disturbances. Comparing these three figures, it can be concluded that when the convergent rate λ is even larger, the steps needed to reach stability is much less. In each figure, when convergent rate λ is determined, more steps are needed to reach stability as the disturbance is much larger. Besides, the influence of λ is more obvious than the size of disturbance.

4.2. Simulation 2- continuous changing slope walking

In the previous section, combining the theoretical explanation of Fig. 7 with the analysis and summary of simulation results in Fig. 6, the fitting result can be obtained as Fig. 8 shown. Then the walking gait transition between different gaits can be realized to complete a more robust and adaptive walking process.

In the situation that $\lambda = 0.5$, $\dot{\theta}_k = -0.5$, $\gamma \in [0.001, 0.040]$, the variation of ϕ_k^- and $\dot{\theta}_k$ during walking process is shown in Fig. 12. As it shows, the first step of this control method is to resist external disturbance. When the disturbance is rejected, the robot can realize passive walking. The second step is to transit gaits according to the changing slope. When the γ is changing, the inter-leg angle ϕ_k^- is also changing under the DCLF-based control method. The value of $\dot{\theta}_k$ varies with the fitting result after the ϕ_k^- is tending towards stability. The gait transition makes the walking process more passive-like and efficient at the basis of stability and robustness.

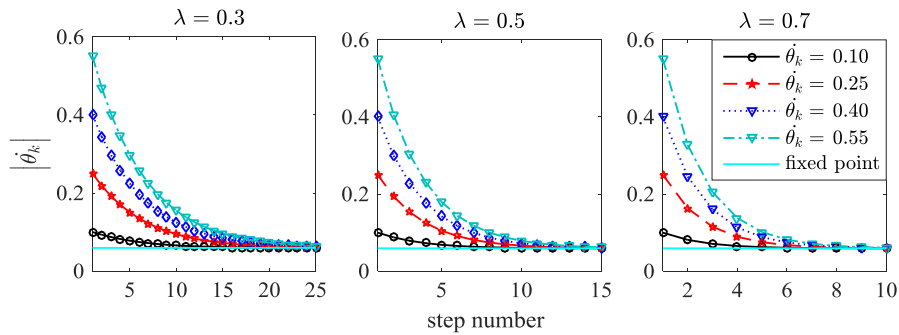


Fig. 11. The impacts of parameters $\dot{\theta}_k$ and λ on stability rate.

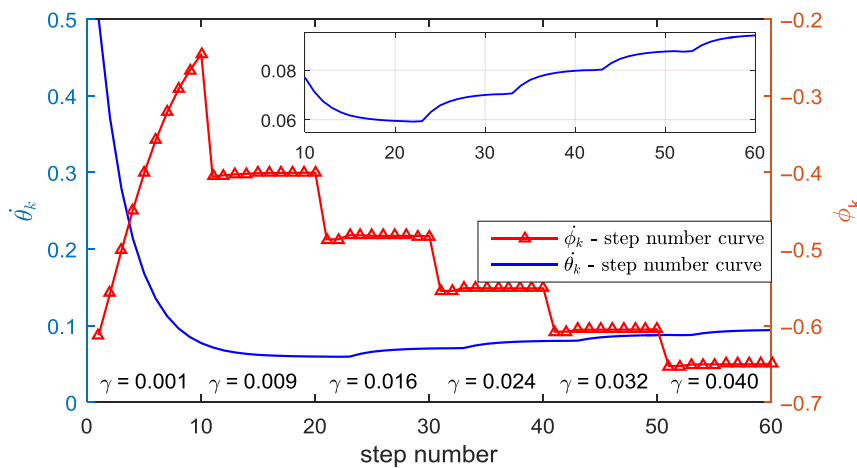


Fig. 12. The variation of $\dot{\phi}_k^-$ and $\dot{\theta}_k$ during walking process with disturbance.

Figure 13 is the variation of the height between swing foot and ground under the same condition with Fig. 12. There are five different gaits in Fig. 13, which is related to the results of Fig. 12. However, some scattered lines are partly below the x -axis, which means the position of swing leg is lower than ground. This result is caused by the large size of disturbance and can be avoided by the bent of knee-joint in practical human walking. In the figure below, there is no scattered line because the disturbance is smaller. Therefore, the phenomenon in the left figure is reasonable and can be avoided by adding knee-joint in future research.

The stick figure under the same disturbance and the same situation is shown in Fig. 14. At the first mid-stance moment, the robot is perturbed. The slope angle is changing for every 5 walking steps from 0.001 to 0.04 rad. As Fig. 14 shown, the robot can resist the disturbance in limited steps and modulate the step length to adapt the variation of the walking environment.

Next, the push-off is considered to realize periodic walking on an uneven ground, whose slope changes from $\gamma = -0.03$ (uphill) to $\gamma = 0$, then to $\gamma = 0.03$ (downhill). In the situation that $\lambda = 0.5$, $\dot{\theta}_k = -0.5$, the push-off can be calculated by the method mentioned in Section 3.4. Then the stick figure of walking robot is shown as Fig. 15.

5. Conclusion

This paper studies the robust and adaptive control method based on the simplest passive walker. The Lyapunov direct method is used to control the crucial state discretely during the walking. Then, the inter-leg angle, related to the step-length, can be obtained to plan the swing leg trajectory from mid-stance to foot-strike. The control torque can be calculated in the light of the dynamic model to reject the disturbance by acting on the hip joint. The gait transition in real-time is proposed by combing the simulation results and theoretical analysis of passive walking. Some simulations are conducted to present that the Lyapunov-based control method can reject disturbance at an exponent rate and then

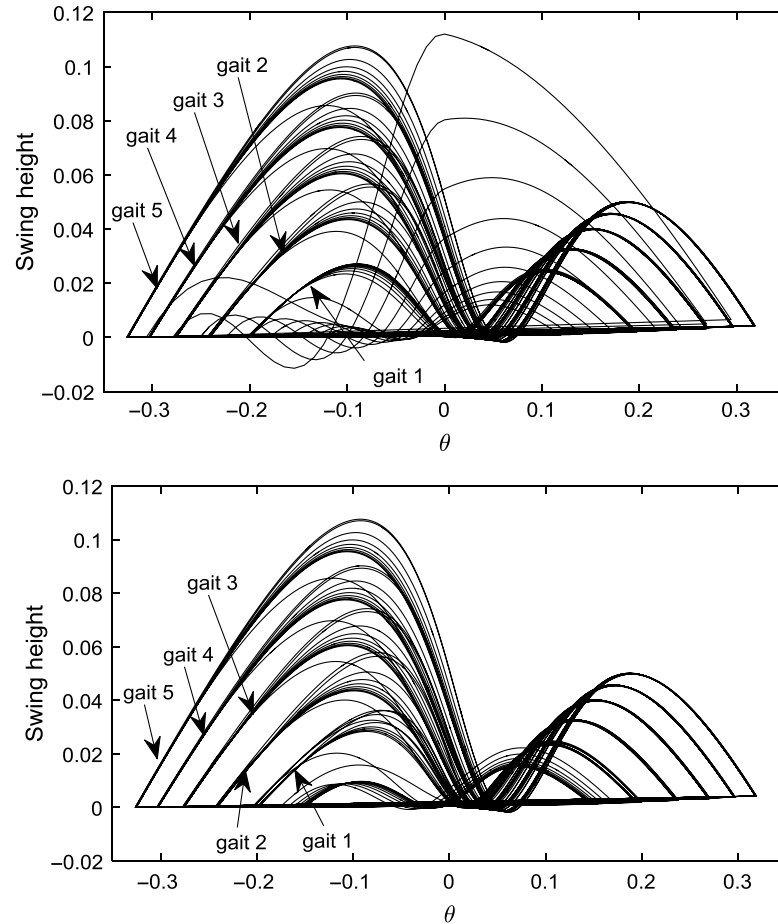


Fig. 13. The swing height when $\dot{\theta}_k = -0.5$ and $\dot{\theta}_k = -0.1$ during 5 gaits.

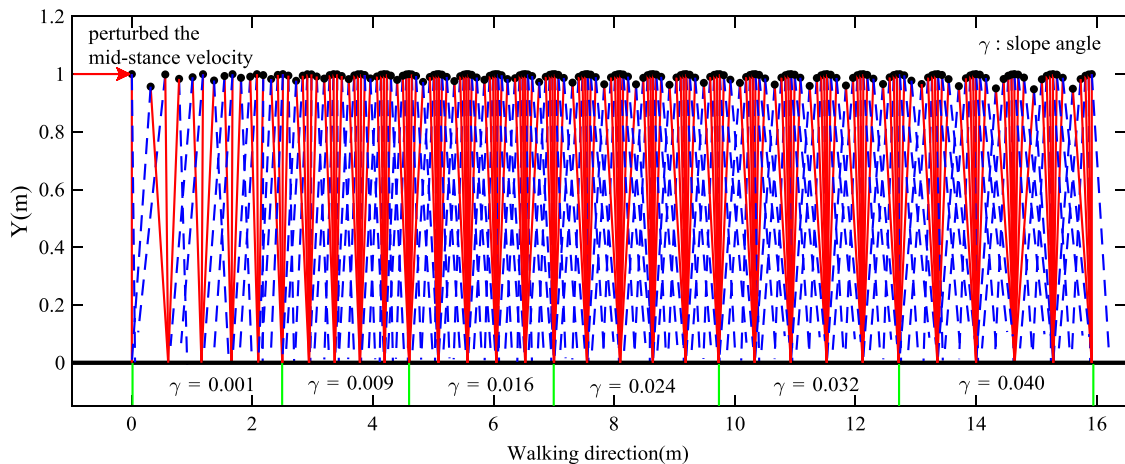


Fig. 14. Stick figure of robot during walking with disturbance on the changing downhill.

guarantee the stability of the system. Moreover, after proving the effectiveness of the Lyapunov-based control algorithm, simulation results prove that the gait transition model is validity to realize a more passive-like and energy-saving walking pattern. The obtained gait can realized more robust and adaptive locomotion than the passive dynamic walking, which is stable only around the fixed point but not energy-consuming.

This work focuses on the simplest model and then proposes the walking control method consisting of Lyapunov-based controller and gait transition module. It has been verified that the robustness

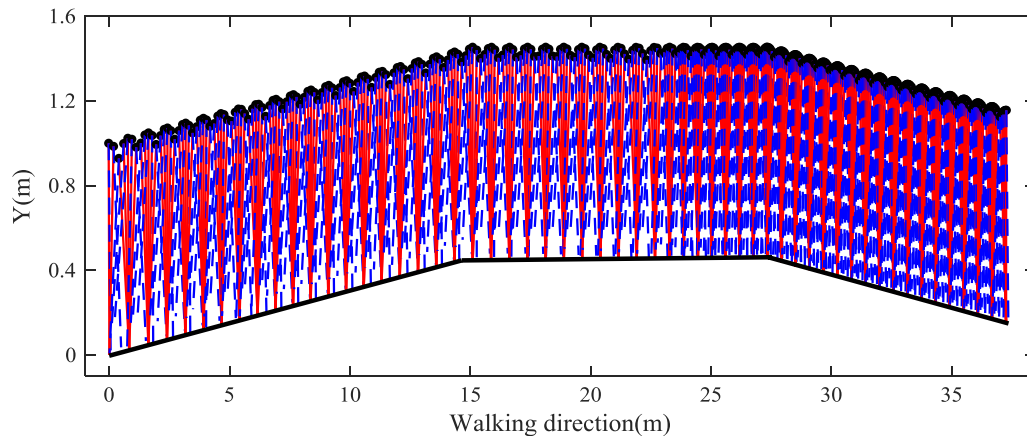


Fig. 15. Stick figure of robot during walking with disturbance on an uneven environment.

and adaptability of biped semi-passive walking can be achieved by using this control method. Theoretically, the presented control method is also suitable for a more complex biped model. The main difference is the dynamic model and some approximate condition related to model. Meanwhile, this work uses the dimensionless parameters, which can make it easy to extend this algorithm to different robot model. Based on the simplest model, the theoretical derivation of this control algorithm is described as explicit as possible. The detailed description of control algorithm is convenient for understanding, analyzing and extending both theoretically and experimentally.

This paper realizes the biped semi-passive walking both on a relatively small slope and on a continuous changing slope (including downhill, flat ground and uphill), respectively. Besides, the biped walking on the level and even on the uphill is also worth studying. The walking on ground with discrete obstacle and even the irregular ground is more common. Therefore, the control method will be optimized and improved to solve these practical problems in the future work to enhance the rapidity of disturbance rejection and the adaptability of the system.

Acknowledgments

This work was supported in part by the National Natural Science Foundation of China (Grant No. U1713211, 61673300) and the Fundamental Research Funds for the Central Universities, Basic Research Project of Shanghai Science and Technology Commission (Grant No. 16JC1401200, 16DZ1200903, 17511108602), and Fundamental Research Funds for the Central Universities and Natural Science Foundation of Jiangsu Province (Grant No. BK20171250). We would like to thank the anonymous reviewers for their valuable suggestions that improved this article.

References

1. X. Y. Yao, H. F. Ding and M. F. Ge, "Task-space tracking control of multi-robot systems with disturbances and uncertainties rejection capability," *Nonlinear Dyn.* **4**, 1–16 (2018).
2. M. Khadiv, S. A. A. Moosavian, A. Yousefikoma and M. Sadedel, "Optimal gait planning for humanoids with 3D structure walking on slippery surfaces," *Robotica* **35**(3), 569–587 (2017).
3. J. W. Grizzle, G. Abba and F. Plestan, "Asymptotically stable walking for biped robots: Analysis via systems with impulse effects," *IEEE Trans. Autom. Contr.* **46**(1), 51–64 (2001).
4. S. J. Hasaneini, J. E. A. Bertram and C. J. B. Macnab, "Energy-optimal relative timing of stance-leg push-off and swing-leg retraction in walking," *Robotica* **35**(3), 654–686 (2017).
5. T. Kinugasa and Y. Sugimoto, "Dynamically and biologically inspired legged locomotion: A review," *J. Robot Mechatron.* **29**(3), 456–470 (2017).
6. A. Zhakatayev, M. Rubagotti and H. A. Varol, "Closed-loop control of variable stiffness actuated robots via nonlinear model predictive control," *IEEE Access* **3**, 235–248 (2017).
7. Q. Huang, K. Yokoi, S. Kajita, K. Kaneko, H. Arai, N. Koyachi and K. Tanie, "Planning walking patterns for a biped robot," *IEEE Trans. Robot. Autom.* **17**(3), 280–289 (2001).
8. T. McGeer, "Passive dynamic walking," *Int. J. Robot. Res.* **9**(9), 62–82 (1990).
9. M. Garcia, A. Chatterjee, A. Ruina and M. Coleman, "The simplest walking model: Stability, complexity, and scaling," *J. Biomech. Eng.* **120**(2), 281 (1998).
10. M. Wisse, A. L. Schwab and F. C. Helm, "Passive dynamic walking model with upper body," *Robotica* **22**(6), 681–688 (2004).

11. M. Wisse, G. Feliksdaal, J. van Frankenhuyzen and B. Moyer, "Passive-based walking robot," *IEEE Robot. Autom. Mag.* **14**(2), 52–62 (2007).
12. K. Hirata and H. Kokame, "Stability Analysis of Linear Systems with State Jump-Motivated by Periodic Motion Control of Passive Walker," *Proceedings of 2003 IEEE Conference on Control Applications*, Taipei, Taiwan (2003).
13. H. Gritli, S. Belghith and N. Khraief, "OGY-based control of chaos in semi-passive dynamic walking of a torso-driven biped robot," *Nonlinear Dyn.* **79**(2), 1363–1384 (2015).
14. H. Gritli and S. Belghith, "Bifurcations and chaos in the semi-passive bipedal dynamic walking model under a modified OGY-based control approach," *Nonlinear Dyn.* **83**(4), 1955–1973 (2016).
15. Y. Huang and Q. Wang, "Torque-stiffness-controlled dynamic walking: Analysis of the behaviors of bipeds with both adaptable joint torque and joint stiffness," *IEEE Robot. Autom. Mag.* **23**(1), 71–82 (2016).
16. Y. Huang, B. Vanderborght, H. R. Van and Q. Wang, "Torque-stiffness-controlled dynamic walking with central pattern generators," *Biol. Cybern.* **108**(6), 803 (2014).
17. Y. Huang, Q. Wang and Q. Wang, "Chaos and bifurcation control of torque-stiffness-controlled dynamic bipedal walking," *IEEE Trans. Syst. Man Cybern. Syst.* **47**(7), 1229–1240 (2017).
18. K. Osuka and Y. Sugimoto, "Stabilization of quasi-passive-dynamic-walking based on delayed feedback control," *Int. Conf. Cont. Autom. Robot. Vis.* **2**, 803–808 (2003).
19. Y. Huang, Y. Gao, B. Chen and Q. Wang, "Adding adaptable stiffness joints to CPG-based dynamic bipedal walking generates human-like gaits," **In: Robot Intelligence Technology and Applications 2, *Advances in Intelligent Systems and Computing***, vol. 274 (J.-H. Kim, E. Matson, H. Myung, P. Xu and F. Karray, eds.) (Springer International Publishing, 2014) pp. 569–580.
20. Y. Huang, L. Chen, B. Vanderborght and Q. Wang, "Transitions of Three Gaits in Dynamic Bipedal Robot with Adaptable Joint Stiffness," *IEEE International Conference on Advanced Intelligent Mechatronics (AIM)*, Busan, Korea (2015) pp. 1–6.
21. E. Borzova and Y. Hurmuzlu, "Passively walking five-link robot," *Automatica* **40**(1), 621–629 (2014). Pergamon Press, Inc.
22. A. Tavakoli and Y. Hurmuzlu, "Robotic locomotion of three generations of a family tree of dynamical systems. Part I: Passive gait patterns," *Nonlinear Dyn.* **73**(3), 1969–1989 (2013).
23. A. Tavakoli and Y. Hurmuzlu, "Robotic locomotion of three generations of a family tree of dynamical systems. Part II: Impulsive control of gait patterns," *Nonlinear Dyn.* **73**(3), 1991–2012 (2013).
24. F. Tan, C. Fu and K. Chen, "Biped Blind Walking on Changing Slope with Reflex Control System," *IEEE International Conference on Robotics and Automation (ICRA)*, Anchorage, Alaska (2010) pp. 1709–1714.
25. C. Fu, "Perturbation Recovery of Biped Walking by Updating the Footstep," *International Conference on Intelligent Robots and Systems (IROS)*, Chicago (2014) pp. 2509–2514.
26. C. Fu, F. Tan and K. Chen, "A simple walking strategy for biped walking based on an intermittent sinusoidal oscillator," *Robotica* **28**(6), 869–884 (2010).
27. P. A. Bhounsule, "Control of a compass gait walker based on energy regulation using ankle push-off and foot placement," *Robotica* **33**(6), 1314–1324 (2015).
28. P. A. Bhounsule, "Foot placement in the simplest slope walker reveals a wide range of walking solutions," *IEEE Trans. Robot.* **30**(5), 1255–1260 (2014).
29. Y. Harata and F. Asano, "Asymptotically Stable and Deadbeat gait Generation of Four-Linked Bipedal Walker by Adjustment Control of Heel Strike Posture," *IEEE-RAS International Conference on Humanoid Robots*, Osaka, Japan (2012) pp. 495–501.
30. P. A. Bhounsule and A. Zamani, "Stable bipedal walking with a swing-leg protraction strategy," *J. Biomech.* **51**, 123–127 (2017).
31. A. Zamani and P. A. Bhounsule, "Foot Placement and Ankle Push-Off Control for the Orbital Stabilization of Bipedal Robots," *IEEE International Conference on Intelligent Robots and Systems (IROS)*, Vancouver, Canada (2017).
32. K. An and Q. Chen, "A passive dynamic walking model based on knee-bend behaviour: Stability and adaptability for walking down steep slopes," *Int. J. Adv. Robot. Syst.* **10**(4), 1–11 (2013).
33. K. An and Q. Chen, "Dynamic optimization of a biped model: Energetic walking gaits with different mechanical and gait parameters," *Adv. Mech. Eng.* **7**(5), 1–13 (2015).
34. K. An, C. Li, Z. Fang and C. Liu, "Efficient walking gait with different speed and step length: Gait strategies discovered by dynamic optimization of a biped model," *J. Mech. Sci. Technol.* **31**(4), 1909–1919 (2017).
35. P. A. Bhounsule and A. Zamani, "A discrete control lyapunov function for exponential orbital stabilization of the simplest walker," *J. Mech. Robot.* **9**(5), 051011 (2017).
36. H. J. Ralston, "Energy-speed relation and optimal speed during level walking," *Int. Z. Angew. Physiol.* **17**(4), 277–283 (1958).
37. R. M. Alexander and G. M. O. Maloiy, "Stride lengths and stride frequencies of primates," *Proc. Zool. Soc. London* **202**(4), 577–582 (1984).